ELSEVIER

Chemical Geology 188 (2002) 171–191

CHEMICAL GEOLOGY
INCLUDING
ISOTOPE GEOSCIENCE

www.elsevier.com/locate/chemgeo

Precise and accurate measurement of ^{226}Ra–^{230}Th–^{238}U disequilibria in volcanic rocks using plasma ionization multicollector mass spectrometry

Aaron J. Pietruszka *, Richard W. Carlson, Erik H. Hauri

Department of Terrestrial Magnetism, Carnegie Institution of Washington, 5241 Broad Branch Road, N.W., Washington, DC 20015, USA

Received 28 June 2001; accepted 28 April 2002

Abstract

We describe analytical techniques for the measurement of ^{226}Ra–^{230}Th–^{238}U disequilibria in volcanic rocks using plasma ionization multicollector mass spectrometry (MC-ICP-MS). Our methods build upon previous MC-ICP-MS techniques for $^{232}Th/^{230}Th$ and $^{238}U/^{234}U$ measurements with the addition of new chemical and/or mass spectrometric procedures for the determination of Th, U and ^{226}Ra abundances. Using sample sizes that are similar to the requirements of state-of-the-art thermal ionization mass spectrometry (TIMS), we are able to measure Th isotope ratios and ^{226}Ra–^{230}Th–^{238}U disequilibria with a precision that is at least ~ 2–$3\times$ better than TIMS and U isotope ratios with a precision that is comparable to TIMS. Replicate analyses of a ^{226}Ra–^{230}Th–^{234}U–^{238}U radioactive equilibrium rock standard (Table Mountain Latite) demonstrate that our MC-ICP-MS techniques are also highly accurate. An additional bonus is that analyses of Ra, Th and U isotope ratios by MC-ICP-MS are much less time-consuming than by TIMS. These analytical improvements will increase the usefulness of U-series isotopes as high-resolution tracers of the nature and timing of magmatic processes at active volcanoes.

Keywords: U-series isotopes; Thorium; Uranium; Radium; Mass spectrometry; Plasma ionization; Volcanic rocks

1. Introduction

Analyses of radioactive disequilibria between the short-lived daughter isotopes of the ^{238}U decay series (e.g., ^{226}Ra, ^{230}Th and ^{234}U) have been used extensively to investigate the nature and timing of magmatic processes at active volcanoes. The primary analytical challenge for these measurements is the precise and accurate determination of the minute quantities of these isotopes in volcanic rocks (e.g., ~ 1 g of a typical Hawaiian basalt contains $< 1\times 10^{-12}$ g ^{226}Ra), which translate to extreme isotope ratios for those elements of the U decay series with a major, naturally occurring isotope (e.g., $^{232}Th/^{230}Th \sim 1$–2×10^5 and $^{238}U/^{234}U \sim 1.8\times 10^4$). Early studies used relatively time-consuming and low precision decay-counting methods to determine the activities (or decay rates) of the U-series isotopes in volcanic rocks (e.g., Somayajulu et al., 1966; Oversby and Gast, 1968). The subsequent development of techniques to directly measure the abundances of these isotopes in geological

* Corresponding author. Present address: Department of Geology, University of Maryland, College Park, MD 20742, USA. Tel.: +1-301-405-0084; fax: +1-301-314-9661.

E-mail address: ajp@geol.umd.edu (A.J. Pietruszka).

0009-2541/02/$ - see front matter © 2002 Elsevier Science B.V. All rights reserved.
PII: S0009-2541(02)00106-7

materials by thermal ionization mass spectrometry (TIMS) significantly improved the accuracy and precision of these measurements and reduced the analysis time compared to the earlier decay-counting methods (e.g., Edwards et al., 1987; Goldstein et al., 1989; Cohen and O'Nions, 1991; Volpe et al., 1991).

Despite the great promise of TIMS methods, a number of analytical problems have limited the effectiveness of U-series isotopes as high-resolution geochemical tracers of magmatic processes. There are two major disadvantages of TIMS techniques for volcanic rocks: (1) the inefficient thermal ionization of Th (<0.1%; Edwards et al., 1987) and, to a lesser extent, U (<0.5%; Yokoyama et al., 2001), and the related difficulty of maintaining a sufficiently large, stable ion beam, result in relatively low signal intensities and poor counting statistics for the minor isotopes, ^{230}Th and ^{234}U, and (2) the lack of enough non-radiogenic isotopes with appropriate relative abundances for Ra, Th and U make it difficult (^{238}U/^{234}U) or impossible (^{232}Th/^{230}Th or ^{226}Ra/^{228}Ra) to simultaneously correct the measured isotope ratios for the effects of instrumental mass fractionation and/or variations in the relative efficiencies of the requisite ion-counting (e.g., Daly) and non-ion-counting (Faraday) detectors (often termed the "Daly–Faraday gain").

Recent studies (e.g., Luo et al., 1997; Turner et al., 2001) have shown that it is possible to precisely measure the extreme Th and U isotope ratios of volcanic rocks using plasma ionization multicollector mass spectrometry (MC-ICP-MS). In a pioneering investigation, Luo et al. (1997) demonstrated a dramatic improvement in the precision of ^{232}Th/^{230}Th (in particular) and ^{238}U/^{234}U measurements by MC-ICP-MS compared to TIMS using relatively large samples of Th and U. Subsequently, Turner et al. (2001) obtained a precision for ^{232}Th/^{230}Th measurements by MC-ICP-MS that is comparable to TIMS using relatively small samples of Th (down to a factor of ~10–20 less than typically used for TIMS). These analytical improvements derive from (1) the much higher sensitivity for Th by MC-ICP-MS (up to ~0.3% in their studies) compared to TIMS and the fact that the intensity of the Th or U ion beam using MC-ICP-MS is directly proportional to concentration of these elements in the sample solution and (2) the ability to easily correct the measured ^{238}U/^{234}U and ^{232}Th/^{230}Th ratios for the effects of instrumental mass fractionation and variations in the Daly–Faraday gain using simultaneous measurements of the ^{238}U/^{235}U ratio (≡137.88) of the sample or a natural U standard solution added to the sample (impossible by TIMS).

The accuracy of these MC-ICP-MS techniques was also evaluated by Luo et al. (1997) and Turner et al. (2001). Most notably, Luo et al. (1997) reported several high-precision ^{238}U/^{234}U analyses of the Pliocene Table Mountain Latite (TML) rock standard and >1 Ga old monazite and zircon crystals that all lie within uncertainty of radioactive equilibrium between ^{234}U and ^{238}U (as would be expected from their old ages compared to the ~245 ka half-life of ^{234}U). This demonstrates that U isotope ratio measurements by MC-ICP-MS can be highly accurate. Both Luo et al. (1997) and Turner et al. (2001) presented ^{232}Th/^{230}Th measurements of solution and rock standards (e.g., TML) that have been frequently analyzed by TIMS and their results agree with previous TIMS measurements within analytical uncertainty. However, it should be noted that these solution standards are not calibrated to the high level of precision achieved by Luo et al. (1997) and TML is thought to be heterogeneous with respect to its Th/U ratio and Th isotopic composition (Williams et al., 1992). A more rigorous test of the accuracy of ^{232}Th/^{230}Th measurements by MC-ICP-MS, such as a complete analysis of a geological material thought to be in radioactive equilibrium between ^{230}Th and ^{238}U (both Th/U and Th isotope ratio measurements are required for this purpose), has never been reported.

In this paper, we describe analytical techniques for the determination of the U-series isotope abundances in volcanic rocks using a VG Elemental Plasma 54-30 (P54-30) plasma ionization multicollector mass spectrometer, which is equipped with a 30-cm electrostatic (energy) filter prior to the ion-counting Daly detector to improve the abundance sensitivity. Our methods build upon the chemical and mass spectrometric procedures outlined by Luo et al. (1997) for ^{232}Th/^{230}Th and ^{238}U/^{234}U measurements by MC-ICP-MS with the addition of new techniques for the determination of Th, U and ^{226}Ra concentrations. We also evaluate the accuracy and precision of our analytical methods using a range of rock (TML and Kil1919) and solution standards (UCSC Th "A" and ZSR Th).

2. Chemistry and mass spectrometry

The chemical and mass spectrometric techniques that we developed are considerably different from those typically used for TIMS analyses of the U-series isotope abundances in volcanic rocks. In this section, we describe our new analytical methods (summarized in Tables 1 and 2) with a comparison to the procedures used by Luo et al. (1997) for $^{232}Th/^{230}Th$ and $^{238}U/^{234}U$ measurements by MC-ICP-MS.

2.1. Sample dissolution

Samples of rock standards (~ 0.5–0.6 g for Kil1919 and 0.05–0.08 g for TML) were digested in a 1:2 mixture of concentrated HF:HNO_3, dried, treated with 8 N HNO_3, dried and heated in 6 N HCl. In order to ensure complete sample-spike equilibration, each sample was centrifuged and any residue was treated with 6 N HCl until dissolved. This clear solution was then dried to a small volume, treated with 8 N HNO_3, dried again to a small volume and diluted to 4 N HNO_3 for splitting and spiking. The small split (for Th and U concentration measurement by isotope dilution) was spiked with calibrated ^{229}Th and ^{233}U tracers and the large split (for Th and U isotope ratio and Ra concentration measurement) was spiked only with a calibrated ^{228}Ra tracer. Finally, each solution was dried completely to equilibrate the sample with the spike(s).

2.2. Thorium, uranium and radium chemistry

Th and U for both isotope dilution and isotope ratio measurements were separated and purified using 0.5-ml columns of Eichrom TRU (TRansUranic) Resin (Horwitz et al., 1993). Our procedure (Table 1) was similar to that of Luo et al. (1997). The sample was loaded onto the pre-cleaned resin in 1.5 N HNO_3. For the Ra cut, this solution and a wash of 1.5 N HNO_3 was collected (along with most of the unwanted major and trace elements). The resin was next washed with 3 N HCl to remove the light to middle rare earth elements. Finally, Th and U were eluted sequentially with 0.2 N HCl and a 0.1 N HCl–0.3 N HF mixture, respectively.

The typical Th and U yields using this procedure were >95% and >85% for the small and large splits, respectively. The Th cuts were essentially free of U, but the U cuts contained a significant amount of Th (U/Th ratios of ~ 4–6) due to the more efficient stripping of Th from the resin in 0.1 N HCl–0.3 N HF compared to 0.2 N HCl (cf., U/Th ratios >100; Luo et al., 1997). However, the presence of Th in the U cut did not affect either the $^{238}U/^{234}U$ or $^{238}U/^{233}U$ measurements (e.g., the ^{232}Th hydride at mass 233 was <0.01% of the signal intensity of ^{233}U for U concentration measurement, which is insignificant). The total procedural blanks were negligible (10–20 pg Th and 6–12 pg U for isotope ratio measurements and 1–4 pg Th and 1–6 pg U for abundance measurements). The minor isotopes of Th and U (^{230}Th or ^{234}U) were below the level of detection in unspiked blanks. The Th cuts were diluted directly off the column and run in a solution of 0.2 N HCl (after the addition of a natural U standard to correct for the effects of the Daly–Faraday gain and/or the instrumental mass fractionation). The U cuts were dried to a small volume (~ 5–10 μl) and diluted with 0.2 N HCl plus a trace amount of HF (<0.01 N). Analyzing Th and U in dilute HCl (with a trace amount of HF for U) maximized the intensity and stability of the ion beam. A variable, low signal intensity (down to a level indistinguishable from the baseline) was observed if Th and U were run in dilute HNO_3 due to chelation between the Th or U and the small amount of extractant from the TRU Resin that bleeds into the sample solution during chemistry (both Th and U partition strongly onto TRU Resin in dilute HNO_3; Horwitz et al., 1993).

To separate and purify Ra (Table 1), we modified the technique of Chabaux et al. (1994). The 1.5 N HNO_3 wash from the Th and U column was dried, dissolved in 1.25 N HCl and loaded onto a 22-ml column of AG50W × 8 cation exchange resin. The column was washed sequentially with 2.5, 4 and 6 N HCl to remove most of the unwanted major and trace elements and ~ 50% of the Ba. The Ra (and the rest of the Ba) was collected in 9 N HCl, dried, treated with concentrated aqua regia, dried, dissolved in 1.25 N HCl and loaded onto a 0.4-ml column of AG50W × 8 cation exchange resin to further purify the Ra and to remove organic material derived from the large cation resin column (which may cause high-mass hydrocarbon interferences with ^{228}Ra and ^{226}Ra). This small cation resin column was washed

Table 1
Summary of the chemical procedures used for the separation and purification of Th, U and Ra

	Th and U separation and purification	
	Reagent	Vol. (ml)
Resin	TRU	0.5
Clean	0.2 N HCl	6
Clean	0.1 N HCl–0.3 N HF	6
Condition	1.5 N HNO_3	6
Load (Collect Ra)	1.5 N HNO_3 (sample)	~ 1–2 (sm. split); ~ 5–10 (lg. split)
Collect Ra	1.5 N HNO_3	6
Wash	3 N HCl	4
Collect Th	0.2 N HCl	4
Collect U	0.1 N HCl–0.3N HF	4

	Ra separation #1		Ra separation #2	
	Reagent	Vol. (ml)	Reagent	Vol. (ml)
Resin	AG50W × 8	22	AG50W × 8	0.4
Clean			6 N HCl	8
Condition	2.5 N HCl	80	2.5 N HCl	4
Load	1.25 N HCl (sample)	6	0.6 N HCl (sample)	1
Wash	2.5 N HCl	100	2.5 N HCl	4.5
Wash	4 N HCl	50		
Wash	6 N HCl	50		
Collect Ra	9 N HCl	60	6 N HCl	5
Clean	9 N HCl	240		

	Ra purification #1/#2		Ra purification #3	
	Reagent	Vol. (ml)	Reagent	Vol. (ml)
Resin	SR/"Pre-filter"	0.4	TRU	0.016
Clean	3 N HNO_3	0.8	0.2 N HCl	0.2
Clean	H_2O	4		
Condition	3 N HNO_3	4	1.5 N HNO_3	0.6
Load (Collect Ra)	3 N HNO_3 (sample)	0.4	1.5 N HNO_3 (sample)	0.05
Collect Ra	3 N HNO_3	2.5	1.5 N HNO_3	0.3

All resin is discarded after a single use (except for Ra separation #1).

with 2.5 N HCl, and the Ra was collected in 6 N HCl, dried and dissolved in 3 N HNO_3. The sample was loaded onto a 0.4-ml column of Eichrom Sr Resin (Horwitz et al., 1992) to separate the Ba from the Ra (Chabaux et al., 1994). Although the presence of Ba does not suppress the signal intensity of Ra by MC-ICP-MS (in direct contrast to TIMS; Volpe et al., 1991; Chabaux et al., 1994), this procedure prevents the contamination of the nebulizer, spray chamber, cones and mass spectrometer with enormous (10s of μg) quantities of Ba and also helps to avoid potential matrix effects on the instrumental mass fractionation (cf., Carlson et al., 2001). Next, the sample was dried, dissolved in 3 N HNO_3 and passed through a 0.4-ml column of Eichrom "pre-filter" resin to remove any organic material derived from the Sr resin (another potential source of high-mass hydrocarbon interferences). Immediately prior to analysis (<2–3 days), any ^{228}Th present in the sample (a natural decay product of and interference with ^{228}Ra) was removed using a 16-μl column of TRU Resin (analogous to the initial 1.5 N HNO_3 Ra cut for the TRU Resin procedure described above). Within this time period, the amount of ingrown ^{228}Th will be <0.1% of the ^{228}Ra (^{228}Ac is calculated to be negligible due to its extremely short half-life of ~ 6.2 h). The efficiency of this Th-elimination step was verified at >99.99% using a mixed ^{232}Th–^{226}Ra solution standard containing Th and Ra concentrations that were similar to a typical sample. It is important to note that the presence

of ^{228}Th in the sample is probably not a problem for TIMS analysis (and is typically ignored) because Th ionizes at a much higher temperature than Ra. Following the last column, the Ra cut was dried to a small volume (~ 5–10 μl), treated with 6 N HCl, dried again to a small volume and diluted with a solution of 0.2 N HCl. Finally, a natural U standard was added to the sample to correct for the effects of instrumental mass fractionation Analyzing Ra in dilute HCl prevented a decrease in the intensity and stability of the U ion beam. The typical Ra yield using this procedure was >95%. The total procedural blanks for ^{226}Ra and ^{228}Ra were below the limits of detection.

2.3. Th, U and ^{226}Ra concentration and ^{232}Th/^{230}Th and ^{238}U/^{234}U analyses

All analyses were performed on the P54-30 at the Carnegie Institution of Washington, which is equipped with a 30-cm electrostatic (energy) filter prior to the ion-counting Daly detector to improve the abundance sensitivity. Additional technical details about this instrument may be found in Halliday et al. (1998) and references therein. Samples were introduced into the system using a desolvating microconcentric nebulizer (Cetac Technologies MCN-6000 or Aridus, hereafter called the MCN) at an uptake rate of ~ 60 ± 10 μl/min. Two different combinations of spray chambers and nebulizers were used: the standard PTFE unit provided by Cetac that runs at a spray chamber temperature of 70 °C and a PFA unit from CPI International that operates at a higher temperature (85 °C) to help prevent droplet formation and, thus, decrease washout time. Typical sensitivities for Th, U and Ra were 0.5 ± 0.1% (cf., < 0.3%; Luo et al., 1997; Turner et al., 2001). This value is greater than, equal to and less than the comparable thermal ionization efficiencies estimated for Th (< 0.1% for >10 ng; Edwards et al., 1987), U (< 0.5% for >10 ng; Yokoyama et al., 2001) and Ra (~ 10–15% for pure standards, but ~ 2× lower for samples; Cohen and O'Nions, 1991), respectively.

The Th and U fractions were run separately on the mass spectrometer. The U abundance was determined by measuring masses 233, 235 and 238 in static mode on the Faraday collectors, with the ^{233}U/^{238}U ratio corrected for instrumental mass fractionation relative to natural ^{238}U/^{235}U (≡ 137.88). The ^{238}U/^{234}U ratio was measured on the large unspiked split using the "multi-static" routine of Luo et al. (1997): two static sequences with masses 234 and 235 measured on the Daly (the latter for Daly–Faraday gain determination) and the ^{238}U/^{234}U ratio corrected for instrumental mass fractionation relative to natural ^{238}U/^{235}U (Table 2). The Th samples were mixed with a U solution prepared from the CRM112 standard, which is a certified reference material from the New Brunswick Laboratory (NBL) with a natural ^{238}U/^{235}U ratio. The Th abundance was determined by measuring masses 229, 232, 235 and 238 in static mode on the Faraday collectors with the ^{229}Th/^{232}Th ratio corrected for instrumental mass fractionation relative to natural

Table 2
Collector positions for ^{232}Th/^{230}Th and ^{238}U/^{234}U ratio and ^{226}Ra concentration measurement by MC-ICP-MS

Element	Sequence	Integration time (s)	Low 2	Low 1	Axial (Daly)	High 1	High 2	High 3	High 4
Thorium	Zero 1	3			229.5	231.5	232.5	234.5	237.5
	Zero 2	3			230.5	232.5	233.5	235.5	238.5
	(1)	12			^{230}Th	^{232}Th		^{235}U	**^{238}U**
	(2)	3			**^{235}U**		^{238}U		
Uranium	Zero 1	3			233.5	234.5	236.5	237.5	
	Zero 2	3			234.5	235.5	237.5	238.5	
	(1)	10			**^{234}U**	^{235}U		^{238}U	
	(2)	3			**^{235}U**		^{238}U		
Radium	Zero	5	218.5	221.5	224.5	231.5	233.5		
	(1)	12			^{226}Ra		**^{235}U**		
	(2)	12			^{228}Ra	**^{235}U**			
	(3)	3	^{235}U	**^{238}U**					

Peak centering for each sequence was performed on the isotopes in **bold**. Zeros were measured once per cycle.

$^{238}U/^{235}U$. The $^{232}Th/^{230}Th$ ratio was measured in the large unspiked split using two static sequences (Table 2) with masses 230 and 235 measured on the Daly (the latter for Daly–Faraday gain determination) and the $^{232}Th/^{230}Th$ ratio corrected for instrumental mass fractionation relative to natural $^{238}U/^{235}U$. In contrast, Luo et al. (1997) measured the minor isotope, ^{234}U, on the Daly to correct for variations in the Daly–Faraday gain. Finally, it should be noted that it was impossible to achieve perfect coincidence of the ion beams in the collectors separated by only 1 amu for both $^{232}Th/^{230}Th$ and $^{238}U/^{234}U$ analyses (Fig. 1). In these cases, the collectors had to be offset slightly to prevent electronic cross talk between them (e.g., High 1 and 2 for Th isotope ratio analysis; Fig. 1). For the isotope ratio measurements, the typical signal intensities were 5.0×10^{-11} A ^{232}Th (using ~ 2.4 ml of a ~ 30–40 ng/g solution) and 3.5×10^{-11} A ^{238}U (using ~ 1.2 ml of a ~ 15–40 ng/g solution), respectively. These correspond to ~ 3×10^{-16} A (1900 cps) of ^{230}Th and ~ 2×10^{-15} A (12,000 cps) of ^{234}U. Analysis times were ~ 40 min for $^{232}Th/^{230}Th$ (~ 60 ratios) and ~ 20 min for $^{238}U/^{234}U$ (~ 30 ratios).

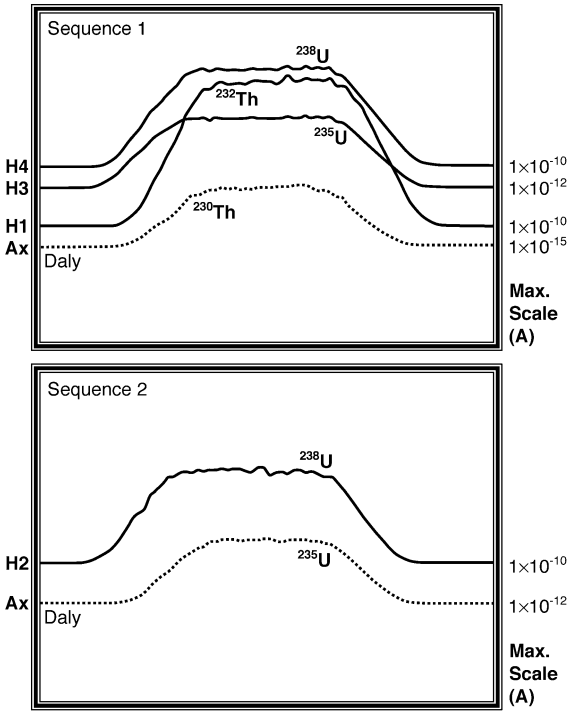

Fig. 1. Scan of the two mass ranges used for $^{232}Th/^{230}Th$ analysis showing the coincidence of the Daly (dashed line) and Faraday (solid lines) detectors. The small wiggles are due to temporal fluctuations of the signal intensity that are inherent to the plasma source. It should be noted that collectors separated by only 1 amu had to be offset slightly to prevent electronic cross talk between them. A similar situation prevails for $^{238}U/^{234}U$ analysis.

A solution of the U standard CRM112 was mixed with the radium sample. The Ra abundance was determined by measuring three static sequences (Table 2) at masses (1) 228 and 235, (2) 226 and 235, and (3) 235 and 238. In this case, only ^{226}Ra and ^{228}Ra were measured on the Daly. The $^{238}U/^{235}U$ ratio from the third sequence was used to correct for instrumental mass fractionation relative to natural $^{238}U/^{235}U$. The Daly–Faraday gain and variations in signal intensity were factored out using the dual ^{235}U measurements of the first two sequences to obtain the $^{226}Ra/^{228}Ra$ ratio. We used ^{235}U for this purpose rather than the major isotope, ^{238}U, because a software limitation prevented the simultaneous measurement of isotope peaks separated by more than 10 amu (e.g., ^{226}Ra to ^{238}U). A third measurement sequence was required to correct for instrumental mass fractionation (rather than using High 1 and 3 to make a $^{238}U/^{235}U$ measurement in the second sequence) because the electronic cross talk due to the 1 amu spacing between High 2 and 3 was unavoidable in the second sequence unless High 3 was no longer coincident with the Axial (Daly) detector. However, it was possible to perfectly optimize the collectors using the $^{226}Ra/^{228}Ra$ scheme shown in Table 2. Typical signal intensities were $1.0–3.6 \times 10^{-16}$ A (620–2200 cps) of ^{226}Ra and $4–8 \times 10^{-17}$ A (250–500 cps) of ^{228}Ra. Radium samples were run to exhaustion over a period of ~ 20 min (~ 20 ratios) using a ~ 1 ml solution of ~ 90–300 fg ^{226}Ra.

2.4. Preparation and calibration of the ^{228}Ra tracer

A ^{228}Ra-enriched tracer was prepared for ^{226}Ra isotope dilution analysis from a ~ 1 mg/g ^{232}Th solution using standard techniques (e.g., Cohen and O'Nions, 1991; Volpe et al., 1991). The initial isotopic composition of this tracer ($^{228}Ra/^{226}Ra = 4.29$) was determined by MC-ICP-MS to ± 0.2% (± $2\sigma_m$; $n = 6$) by correcting the $^{228}Ra/^{226}Ra$ ratios measured over a ~ 2-year period for the effects of ^{228}Ra and ^{226}Ra decay ($\lambda^{228}Ra = 0.1205$ year^{-1} and $\lambda^{226}Ra = 4.332 \times 10^{-4}$ year^{-1}; Tuli, 2000). Immediately prior

to analysis (<2–3 days), each of these aliquots were passed through a 16-μl column of TRU Resin to remove any ^{228}Th present in the solution. The temporal ^{228}Ra/^{226}Ra evolution of our ^{228}Ra tracer lies within analytical uncertainty of the trend expected for pure ^{228}Ra and ^{226}Ra decay without interference from either ^{228}Th or ^{228}Ac. The ^{228}Ra tracer was calibrated against the National Institute of Standards and Technology (NIST) ^{226}Ra standard SRM4966, which has an overall concentration uncertainty of 1.2%. Mass spectrometric analysis of this standard showed that it was essentially pure ^{226}Ra (^{226}Ra/^{228}Ra>10^4). Measurements of seven different mixtures of our ^{226}Ra standard and ^{228}Ra tracer (also passed through TRU Resin immediately prior to analysis) gave spike concentrations that agree to $\pm 0.2\%$ ($\pm 2\sigma_m$), which is $\sim 6\times$ better than its overall accuracy.

2.5. Calibration of the Daly detector

All of our ^{232}Th/^{230}Th, ^{238}U/^{234}U and ^{226}Ra/^{228}Ra analyses use the ion-counting Daly detector. Isotope ratios measured using a Daly are influenced by a number of instrumental parameters, such as the dead time and the voltages on the Daly knob and photomultiplier tube (PMT). Thus, it is critical to calibrate the Daly (like any ion-counting system) to produce accurate results for these isotope ratio measurements.

For this purpose, we used a solution of the U standard CRM112. Although this standard has a natural ^{238}U/^{235}U ratio, its ^{235}U/^{234}U ratio was unknown prior to this study. Since the ^{235}U/^{234}U ratio must be known to calibrate the Daly, we measured the isotopic composition of CRM112 solely on the Faraday collectors using two solutions with different U concentrations. First, the ^{238}U/^{235}U ratio was measured in a relatively dilute solution to determine the magnitude of the instrumental mass fractionation. Second, the ^{235}U/^{234}U ratio was measured in a relatively concentrated solution with the Faraday collectors positioned to avoid the large ^{238}U ion beam (^{234}U in High 3 and ^{235}U in High 4). Third, the ^{238}U/^{235}U ratio was again measured in the dilute solution. The measured ^{235}U/^{234}U ratio was corrected for instrumental mass fractionation using the average of the two ^{238}U/^{235}U analyses. The ^{234}U signal intensities ranged from 8 to 20×10^{-15} A for these measurements. Four analyses of CRM112 using only the Faraday collectors gave a mean ^{235}U/^{234}U = 135.50 ± 0.08 ($\pm 2\sigma_m$), which we adopt as the "true" value for this standard. It should be noted that this value is considerably different from the ^{235}U/^{234}U ratio of the commonly used NBL U standard CRM112-A (^{235}U/^{234}U ~ 137.2; Cheng et al., 2000), which is a completely different standard that was formerly issued by the NIST as SRM960. The origin of the difference in the abundance of ^{234}U between these U standards is unknown.

Given this result, we measured the ^{235}U/^{234}U ratio of CRM112 on the Daly and adjusted the voltages on the Daly knob and PMT (1) to obtain the closest possible approach to the expected ^{235}U/^{234}U ratio, (2) to preserve a flat-topped shape to the signal peaks on the Daly (Fig. 1) and (3) to minimize any background noise on the Daly baseline. This procedure was followed by a measurement of the Daly dead time. The dead time was set to 0 ns in the software (i.e., no correction for dead time) and the apparent Daly–Faraday gain (a direct comparison of the ^{235}U signal intensity between the Daly and the Faraday detectors) was measured at a range of signal intensities. The apparent decrease in the Daly–Faraday gain as the signal intensity of ^{235}U increases provides a direct estimate of the dead time, which was calculated from the best-fit line on a plot of the Daly–Faraday gain vs. the intensity of the ^{235}U signal on the Daly (dead time = − slope/intercept). After setting the dead time, the linearity of the Daly was verified by measuring the ^{235}U/^{234}U ratio of CRM112 at a range of solution concentrations (and, thus, signal intensities of ^{235}U on the Daly). The Daly was checked before every Th, U and Ra isotope ratio analysis session and this entire procedure was repeated as necessary to maintain accurate and linear results.

Despite our calibration and monitoring of the Daly, we observed a distinct drift in the ^{235}U/^{234}U ratios of CRM112 during the last ~ 3 years (Fig. 2). Although there is no simple 1:1 trend, the major changes in the ^{235}U/^{234}U ratio of CRM112 seem to correlate with shifts in the Daly–Faraday gain (despite the fact that the effect of this gain on the ^{235}U/^{234}U ratio is corrected during analysis). This suggests that the temporal variation in the ^{235}U/^{234}U ratio of CRM112 is related to changes in the performance of the Daly detector rather than other analytical causes, although the exact origin is unknown. Indeed, the relatively large offsets in the ^{235}U/^{234}U ratio correlated with

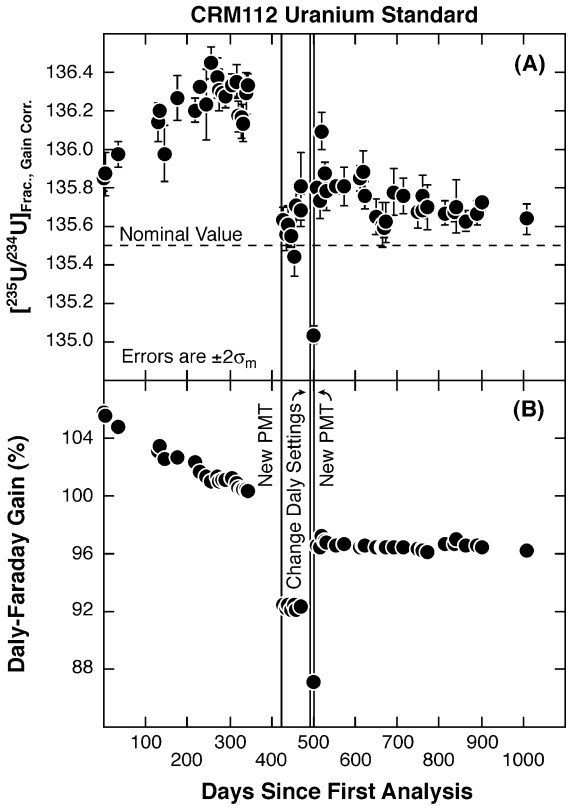

Fig. 2. Temporal variations of (A) the $^{235}U/^{234}U$ ratio of CRM112 and (B) the Daly–Faraday gain. Each data point represents the average of at least three measurements. The Daly settings were adjusted after ~ 500 days to temporarily solve a problem with baseline noise. The problem was fixed permanently by replacing the photomultiplier tube (PMT). The $\pm 2\sigma_m$ uncertainties on the mean Daly–Faraday gain values are similar to or smaller than the size of the symbols.

major changes to the ion-counting system (PMT replacements) or a relatively large adjustment made to the Daly settings to temporarily solve a problem with background noise (Fig. 2).

This range in the performance of the Daly (reflected by variations in the $^{235}U/^{234}U$ ratio of CRM112) also affected the $^{232}Th/^{230}Th$ and $^{238}U/^{234}U$ ratios of unknowns. Our approach to correct for this effect was to normalize all $^{232}Th/^{230}Th$ and $^{238}U/^{234}U$ (via $^{235}U/^{234}U$) analyses of unknowns to the nominal $^{235}U/^{234}U$ value for CRM112, which was measured repeatedly before and after every analytical session. The CRM112 standard was used to normalize the $^{232}Th/^{230}Th$ analyses rather than a Th isotope ratio standard to avoid losing information on the accuracy and precision of our $^{232}Th/^{230}Th$ measurements. This simple correction dramatically improved the long-term reproducibility of both the $^{232}Th/^{230}Th$ and $^{238}U/^{234}U$ measurements by a factor of ~ 2 (and, thus, appears to be independent of the 2 vs. 1 amu mass differences between the $^{232}Th/^{230}Th$ and $^{235}U/^{234}U$ ratios). The $^{226}Ra/^{228}Ra$ ratios were not corrected for this effect because the normalization (1) did not change the reproducibility of rock standards (which were all analyzed during a period of relatively constant $^{235}U/^{234}U$ ratios for CRM112), (2) decreased the reproducibility of our age-corrected measurements of the $^{226}Ra/^{228}Ra$ ratio and concentration of our ^{228}Ra tracer by a factor of ~ 2 and (3) caused the temporal $^{228}Ra/^{226}Ra$ evolution of our ^{228}Ra tracer to deviate significantly from the expected trend based on the accepted decay constants for ^{228}Ra and ^{226}Ra (Tuli, 2000). The origin of this difference between Ra vs. Th and U is unknown, but may reflect an additional bias due to the relatively large intensity of the ^{235}U ion beam measured on the Daly detector for $^{232}Th/^{230}Th$ and $^{238}U/^{234}U$ analyses.

2.6. Isobaric interferences

Isobaric interferences are potentially a major source of error on the $^{232}Th/^{230}Th$, $^{238}U/^{234}U$ and $^{226}Ra/^{228}Ra$ ratios because the typical signal intensities of ^{226}Ra, ^{228}Ra, ^{230}Th and ^{234}U are so low. In this study, we observed two types of isobaric interferences in the Ra, Th and U mass range: (1) interferences that appear to be related to the sample introduction portion of the mass spectrometer and (2) interferences related to the chemical separation and purification of Ra, Th and U. The effects of the former type of interferences were corrected by direct measurement (an on-peak baseline subtraction), whereas the latter type of interferences were removed by chemical methods.

The first type of isobaric interferences manifested as minor (usually $\leq 1 \times 10^{-18}$ A or 6 cps), but distinct, peaks at virtually every mass in the Ra, Th and U mass range (Fig. 3). These interferences are difficult to identify, but the proportions of the peaks show that they are neither elemental interferences (e.g., the peaks at masses 234, 235 and 238 do not match the natural abundances of uranium; Fig. 3) nor

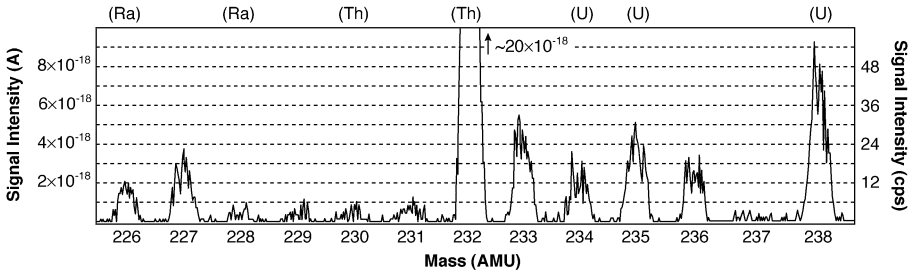

Fig. 3. Baseline scan of the Ra, Th and U mass range showing the small, but distinct, isobaric interferences that are thought to be high-mass hydrocarbons that survive the high temperature of the plasma source. The interference peaks observed during this particular analytical session were much larger than typically observed (usually $\leq 1 \times 10^{-18}$ or 6 cps) and were subsequently reduced to normal levels by cleaning the interior of the desolvating microconcentric nebulizer (MCN). The larger peaks at masses 232 and 238 are due mostly to the presence of ^{232}Th and ^{238}U in the wash solution and/or MCN.

simple molecular interferences (e.g., oxides or hydrides). Instead, our best explanation is that these small peaks are high-mass hydrocarbons derived from a number of sources related to the sample introduction portion of the mass spectrometer, such as organic material introduced with the argon supply, released from the surface of the cones or retained in the MCN from previous samples. Over the long term (days to months), the magnitude and proportions of the peaks were variable. However, we found that the worst of the interferences could be eliminated by installing clean cones, changing to a new Ar tank and/or cleaning the interior of the MCN with 0.5 N HNO_3. Over the short term (hours), the magnitude and proportions of the peaks tended to be fairly constant. Thus, we simply made an on-peak background correction for any interferences before every Ra, Th and U isotope ratio measurement. For Ra and Th, this was done by measuring masses 226 and 228 or 230 using a solution of CRM112 (for the purpose of peak centering) that was previously purified using standard anion exchange chemistry and verified to be free of ^{226}Ra, ^{228}Ra or ^{230}Th. The interferences for ^{234}U were usually negligible (due to the relatively large signal intensities for ^{234}U), but a clean wash solution (0.2 N HCl with a trace amount of HF) was used when a correction was necessary. The typical intensities of these interferences were: 226 ($< 8 \times 10^{-20}$ A or 0.5 cps), 228 ($< 1 \times 10^{-19}$ A or 0.9 cps), 230 ($< 7 \times 10^{-19}$ A or 4 cps) and 234 ($< 2 \times 10^{-19}$ A or 1 cps). In all cases, the magnitude of the background correction was $< 0.2\%$ (similar to or less than the $\pm 2\sigma$ uncertainty of our measurements).

The second type of isobaric interferences were identified as high-mass hydrocarbons derived from organic material that bleeds into the sample solutions from the resins used for the chemical separation and purification of Ra, Th and U (Fig. 4). Isobaric interferences at masses 226 and 228 in samples passed through Sr Resin are frequently observed during TIMS analysis of Ra prior to thermal degassing of the sample in the mass spectrometer. Although it may be surprising that such hydrocarbons (and those described previously) can survive the high temperature of the plasma source, we note that the hydrocarbon peaks observed using MC-ICP-MS are several orders of magnitude smaller than those observed during the initial low-temperature degassing stage of Ra analysis by TIMS. In any case, we characterized the potential interferences at masses 226, 228, 230 and 234 by analyzing unspiked blank solutions that had been passed through the same chemical procedures as the samples. For the Th cut, no interference at mass 230 was detected as long as the blank solutions were analyzed in dilute HCl (Fig. 4). In contrast, distinct peaks at mass 230 became apparent if even a trace amount of HF was added to the Th solution. Although the U cut was free of any interference at mass 234, this solution typically contained a significant peak at mass 230 (Fig. 4). Thus, a sample's U cut could not be re-mixed with its Th cut after chemistry to correct the measured ^{232}Th/^{230}Th ratio for the effects of instrumental mass fractionation and Daly–Faraday gain (cf., Luo et al., 1997). Instead, it was necessary to use a U solution standard, such as CRM112, to avoid this problem. For Ra, interferences

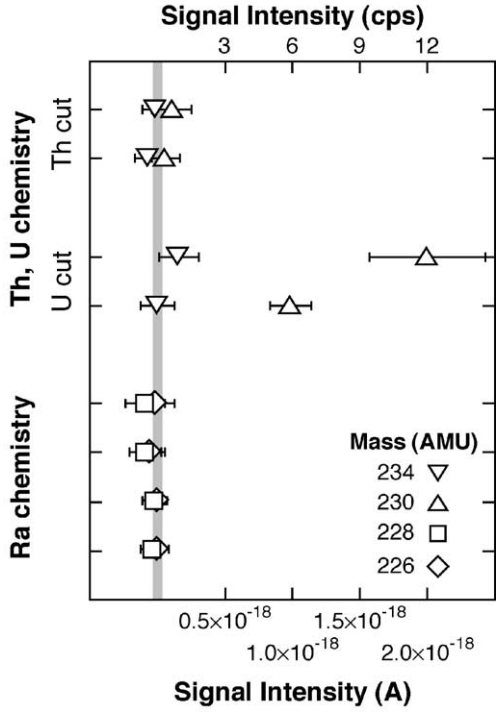

Fig. 4. Measurements of the potential isobaric interferences in blank solutions run through the total chemical procedure for Ra, Th and U. Any interferences at masses 226, 228, 230 and 234 that derive from the chemical separation and purification of Ra, Th and U are negligible (the interference at mass 230 in the U cut does not affect the $^{238}U/^{234}U$ measurement). The error bars are the within-run $\pm 2\sigma_m$ uncertainties.

were observed at masses 226 and 228 only in blank solutions passed through the initial 0.5-ml TRU Resin column or the 22-ml cation resin column. However, these interferences were effectively removed (Fig. 4) when the blank solution was subsequently passed through the 0.4-ml cation resin column (interferences from the final 16-μl TRU Resin column were below the limits of detection). Thus, we conclude that any interferences at masses 226, 228, 230 and 234 derived from the chemical separation and purification of Ra, Th and U had a negligible effect on the $^{232}Th/^{230}Th$, $^{238}U/^{234}U$ and $^{226}Ra/^{228}Ra$ ratios.

2.7. Memory effects

We used the following washout procedures after every sample. For Th and U, a sequential wash of 0.5 N HNO_3, 0.2 N HCl and 0.2 N HCl with a trace amount of HF (< 0.01 N) was repeated until the ^{232}Th and ^{238}U signal intensities decayed to an insignificant level (< 0.01% of the anticipated signal intensity of the next sample). The 0.2 N HCl–trace HF solution was particularly effective at removing Th and U from the system, but we minimized its use during $^{232}Th/^{230}Th$ analysis because the HF sometimes caused an increase in the magnitude of the isobaric interference at mass 230. For Ra, a sequential wash of 0.5 N HNO_3 and 0.2 N HCl was used. The 0.2 N HCl–trace HF solution was not used for Ra because it did not significantly improve the washout and sometimes caused an increase in the magnitude of the isobaric interferences at masses 226 and 228. In all cases, the MCN was conditioned with a solution identical to that of the sample prior to analysis. In general, it took the following times to wash the MCN after a sample: Th (~ 20–40 min), U (~ 10–20 min) and Ra (~ 10–20 min). The amount of time required depended strongly on the type of spray chamber and nebulizer used with the MCN. Washout was substantially faster (a factor of ~ 2) using the PFA unit compared to the PTFE unit. Thus, the total amount of time required for a Th, U or Ra isotope ratio analysis by MC-ICP-MS (including washout) was ~ 60–80 min for $^{232}Th/^{230}Th$, ~ 30–40 min for $^{238}U/^{234}U$ and ~ 30–40 min for $^{226}Ra/^{228}Ra$. In each case, this is much faster than the typical amount of time required for a similar analysis by TIMS (≫1 h).

2.8. Abundance sensitivity

High abundance sensitivity is critical for our $^{232}Th/^{230}Th$, $^{238}U/^{234}U$ and $^{226}Ra/^{228}Ra$ measurements. During this study, the abundance sensitivity at the Daly detector ranged between 0.4 and 0.9 ppm (typically ~ 0.5 ppm) at 1 amu lower than mass 238 (measured using CRM112; Fig. 5), which is a factor of ~ 5–10 × better than observed at the Faraday detector prior to the 30-cm electrostatic (energy) filter. At this level of abundance sensitivity, we found that the contribution of the ^{238}U tail to ^{226}Ra, ^{228}Ra and ^{230}Th was negligible due to the relatively large mass spacing between them. The ^{238}U tail under mass 234 was relatively small, but significant (< 0.1%). Thus, the baseline correction for $^{238}U/^{234}U$ analysis was performed using the average of two baseline measurements at ± 0.5 amu around mass 234 (Table

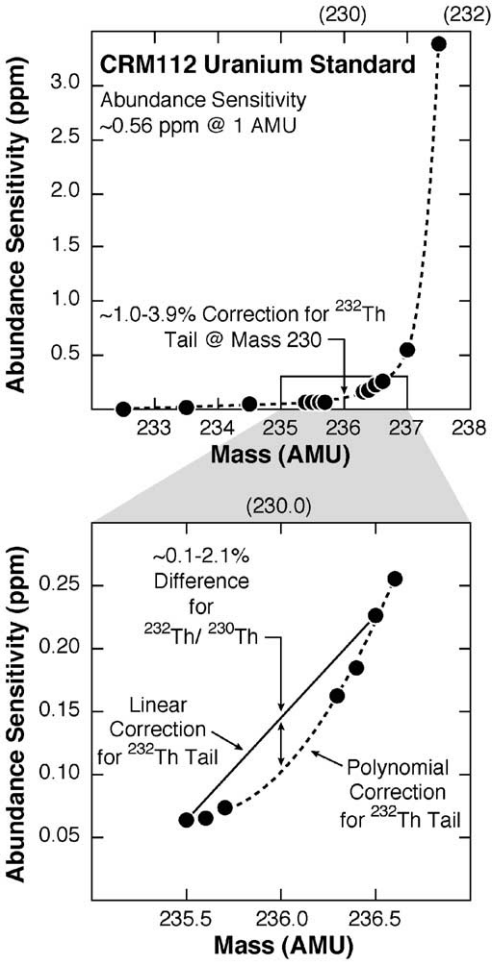

Fig. 5. Abundance sensitivity profile using the CRM112 U standard as an analogue of the "tail" correction required for accurate $^{232}Th/^{230}Th$ measurements. We found that a baseline correction based on the fit of a 3rd-order polynomial to the "shape" of the tail provided more accurate results for $^{232}Th/^{230}Th$ ratios. The signal intensity of ^{238}U was $\sim 4 \times 10^{-11}$ A during this measurement. The within-run $\pm 2\sigma_m$ uncertainties are less than the size of the symbols.

2). In contrast, the proportion of the ^{232}Th tail below mass 230 was relatively large due to the smaller mass spacing and lower intensity of the ^{230}Th ion beam. For the $^{232}Th/^{230}Th$ ratios measured in this study, the ^{232}Th tail at mass 230 ranged between $\sim$ 1.0% and 3.9% of the signal intensity of ^{230}Th. Luo et al. (1997) corrected for this effect using the average of two baseline measurements at $\pm$ 0.5 amu around mass 230, analogous to our correction for ^{234}U. Although this type of baseline correction is adequate for $^{238}U/^{234}U$ measurement, detailed scans showed that the "shape" of the tail is distinctly non-linear at 2 amu lower than the major isotope peak (Fig. 5). We found that a 3rd-order polynomial gave the best fit to the overall shape of the tail. Thus, the linear baseline correction used by Luo et al. (1997) for $^{232}Th/^{230}Th$ analysis was not valid in our case. Instead, we measured the shape of the tail using U from CRM112 (as an analogue to ^{232}Th) at the start of each $^{232}Th/^{230}Th$ analysis session. Although the shape of the tail varied significantly from session to session, we found that it remained relatively constant over short periods of time (days). Using a software correction, 2 baselines measured at $\pm$ 0.5 amu around mass 230 (Table 2) were weighted in appropriate proportions based on the shape of the tail to approximate the true baseline below ^{230}Th. This correction made a $\sim$ 0.1–2.1% difference in the final $^{232}Th/^{230}Th$ ratios of the standards measured in this study. This approach is similar to the exponential fit employed by McDermott et al. (1993) to correct their measured $^{232}Th/^{230}Th$ ratios for a much larger ($\sim$ 15%) tail using a TIMS that lacked an energy filter prior to the ion-counting detector.

2.9. An evaluation of the correction for instrumental mass fractionation

The instrumental mass fractionation induced by MC-ICP-MS is relatively large ($\sim$ 0.5–0.9%/amu for U) compared to TIMS and must be corrected to obtain accurate and precise results. Corrections to the $^{238}U/^{234}U$ and $^{238}U/^{233}U$ ratios are straightforward because U has two non-radiogenic isotopes ($^{238}U/^{235}U \equiv 137.88$) and, thus, the exponential mass fractionation law of Russell et al. (1978) may be used. For the $^{232}Th/^{230}Th$, $^{232}Th/^{229}Th$ and $^{226}Ra/^{228}Ra$ ratios, we used an internal inter-element correction for instrumental mass fractionation (U from CRM112). Although inter-element fractionation in the MC-ICP-MS is sometimes assumed to be simply mass dependent (e.g., Walder et al., 1993), detailed studies of the isotope systematics of Pb–Tl (White et al., 2000), Cu–Zn (Maréchal et al., 1999) and Pd–Ag (Carlson et al., 2001) have found small, but significant, departures from mass-dependent fractionation between elements of similar mass. It is currently impossible to evaluate the inter-element fractionation behavior of U and Ra because the $^{226}Ra/^{228}Ra$ ratio must be meas-

ured using very low signal intensities on the Daly (due to the low concentrations of our ^{226}Ra standard and ^{228}Ra tracer) and, thus, the analytical uncertainties are too large to distinguish small departures from mass-dependant fractionation. Therefore, we assumed that the instrumental mass fractionation between U and Ra is simply mass dependent. Similarly, it is difficult to evaluate the inter-element fractionation behavior of Th and U because there is only one major, naturally occurring isotope of Th. However, we were able to examine several aspects of the inter-element fractionation behavior of Th and U using U from CRM112 and two different mixtures of our ^{232}Th standard and ^{229}Th tracer.

According to the exponential mass fractionation law of Russell et al. (1978)

$$R^{\mathrm{Th}}_{\mathrm{Meas.}} = R^{\mathrm{Th}}_{\mathrm{Frac.\,Corr.}} \left(\frac{M^{232}\mathrm{Th}}{M^{229}\mathrm{Th}}\right)^{\beta_{\mathrm{Th}}}, \quad (1)$$

where $R^{\mathrm{Th}} = {}^{232}\mathrm{Th}/{}^{229}\mathrm{Th}$, M is the mass of the isotope (in amu), and β is the fractionation factor. The "Meas." and "Frac. Corr." subscripts refer to the measured and fractionation-corrected (or "true") isotope ratios, respectively. A similar equation can be written for U. These two equations may be combined and rearranged to produce an expression that is useful for evaluating inter-element instrumental mass fractionation (e.g., Maréchal et al., 1999; White et al., 2000):

$$\ln R^{\mathrm{Th}}_{\mathrm{Meas.}} = \frac{\beta_{\mathrm{Th}}}{\beta_{\mathrm{U}}} \frac{\ln\left(\frac{M^{232}\mathrm{Th}}{M^{229}\mathrm{Th}}\right)}{\ln\left(\frac{M^{238}\mathrm{U}}{M^{235}\mathrm{U}}\right)} \ln R^{U}_{\mathrm{Meas.}} + \left[\ln R^{\mathrm{Th}}_{\mathrm{Frac.\ Corr.}} - \frac{\beta_{\mathrm{Th}}}{\beta_{\mathrm{U}}} \frac{\ln\left(\frac{M^{232}\mathrm{Th}}{M^{229}\mathrm{Th}}\right)}{\ln\left(\frac{M^{238}\mathrm{U}}{M^{235}\mathrm{U}}\right)} \ln R^{\mathrm{U}}_{\mathrm{Frac.\ Corr.}}\right]. \quad (2)$$

This equation has the form of a straight line on a plot of the natural logarithms of the measured ^{232}Th/^{229}Th and ^{238}U/^{235}U ratios with a slope given by

$$\frac{\beta_{\mathrm{Th}}}{\beta_{\mathrm{U}}} \frac{\ln\left(\frac{M^{232}\mathrm{Th}}{M^{229}\mathrm{Th}}\right)}{\ln\left(\frac{M^{238}\mathrm{U}}{M^{235}\mathrm{U}}\right)}. \quad (3)$$

If the inter-element instrumental mass fractionation between Th and U is simply mass dependent, then $\beta_{\mathrm{Th}} = \beta_{\mathrm{U}}$ and the observed slope is a function only of the relative masses of the isotopes (e.g., Maréchal et al., 1999; White et al., 2000).

This relationship was tested experimentally using a Th solution with a ^{232}Th/^{229}Th ratio of ~ 4 (Fig. 6A). U from CRM112 was added to this solution in variable proportions to simulate the range of Th/U ratios in our unknowns (for both Th concentration and ^{232}Th/^{230}Th ratio measurements). These mixtures were run on two separate analytical sessions using only the Faraday collectors. Fortunately, the two sessions displayed slightly different and variable fractionation factors ($\sim 0.73-0.75\%$ and $0.77-0.83\%$ amu^{-1} for U). Overall, a plot of the measured ln[^{232}Th/^{229}Th] vs. ln[^{238}U/^{235}U] shows a linear trend ($r^2 = 0.94$). However, the slope of the data on this plot (0.9 ± 0.1, 2σ) does not quite equal the value expected from the relative masses of the isotopes (1.03). This indicates that, in fact, $\beta_{\mathrm{Th}} \neq \beta_{\mathrm{U}}$. A more detailed examination of the data reveals a correlation between either the fractionation-corrected or measured ^{232}Th/^{229}Th ratios and the measured Th/U ratio of the solution (Fig. 6B). The ^{232}Th/^{229}Th ratio increases slightly as the Th/U ratio increases ($\sim 0.011 \pm 0.003\%$ amu^{-1}, 2σ, for every unit increase in Th/U). This indicates the presence of a relatively small matrix effect on Th and U fractionation (cf., Pd–Ag matrix effects; Carlson et al., 2001). As the relative concentration of Th (or Th/U ratio) in the solution increases, the fractionation factor measured using U becomes a greater underestimate of the actual Th fractionation.

To correct for this matrix effect, all ^{232}Th/^{229}Th and ^{232}Th/^{230}Th measurements in this study were normalized to Th/U = 0 using the relationship in Fig. 6B, which seems to represent the limit of purely mass dependant inter-element instrumental mass fractionation for Th–U mixtures. The validity of this correction was verified in two ways. First, the measured ^{232}Th/^{229}Th ratios from the previous experiment (which were determined at a relatively large range in Th/U) were normalized to Th/U = 0 and plotted again in Fig. 6A. The normalized data show a better linear trend ($r^2 = 0.98$) with a slope that lies within uncertainty of the value expected from the relative masses of the isotopes (1.04 ± 0.06, 2σ). Second, we performed another experiment using a Th solution

with a $^{232}Th/^{229}Th$ ratio of ~ 12 (Fig. 6C). Two portions of this solution were run using only the Faraday collectors: one that contained only Th and one that had U from CRM112 added to give a Th/U ratio of ~ 0.8. The mixed Th–U solution was run in the same fashion as the solution from the first experiment with the final $^{232}Th/^{229}Th$ ratios normalized to Th/U = 0. For the U-free Th solution, the fractionation factor was measured using U from CRM112 before and after each analysis. In this case, the $^{232}Th/^{229}Th$ of the U-free solution was corrected for the effects of instrumental mass fractionation using the average of the two $^{238}U/^{235}U$ ratios. The average fractionation-corrected $^{232}Th/^{229}Th$ ratios of these two types of measurements are identical within uncertainty (< 0.01% different), which demonstrates the validity of our correction for the Th–U matrix effect. In any case, it is important to note that the magnitude of the matrix effect that we observed for Th (< 0.03%/amu) is insignificant given the current analytical uncertainty of our techniques. However, a correction for this effect will be critical for future studies that improve

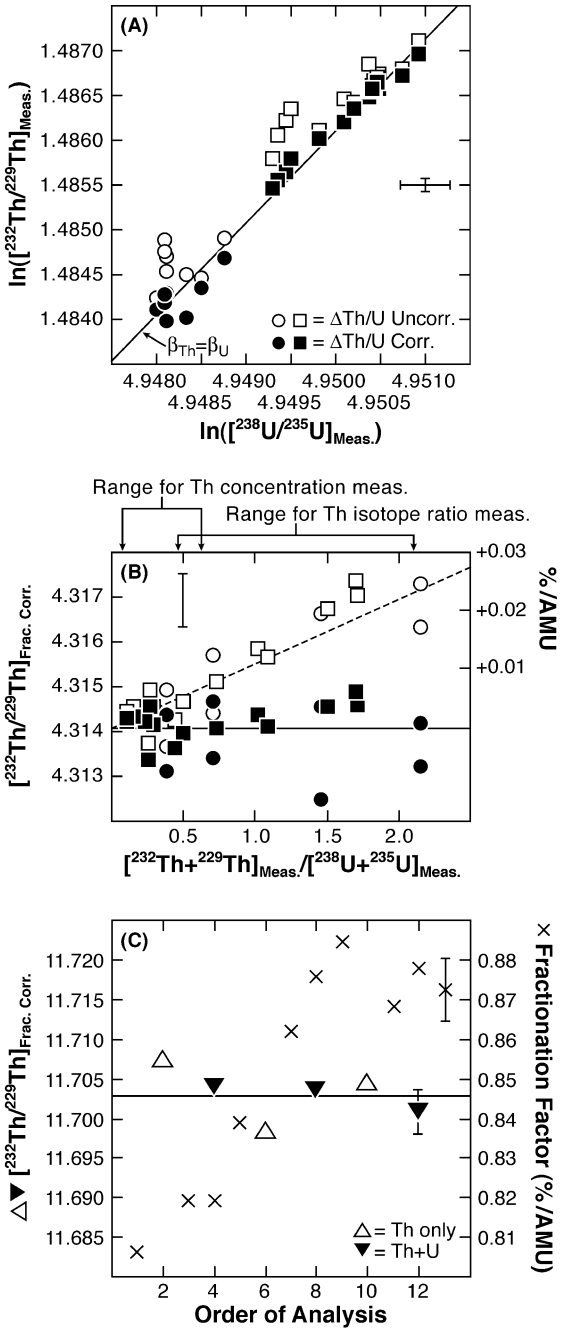

Fig. 6. An evaluation of inter-element instrumental mass fractionation effects for Th and U. (A) A plot of the natural logarithms of the measured $^{232}Th/^{229}Th$ vs. $^{238}U/^{235}U$ ratios of mixed Th–U solutions with variable Th/U ratios and a constant $^{232}Th/^{229}Th$ ratio of ~ 4. Data were collected during two separate analytical sessions that displayed slightly different fractionation factors (circles vs. squares). The raw data (open symbols) have a slope that is significantly different from the slope expected from the relative masses of the isotopes (line of $\beta_{Th} = \beta_U$), which indicates that the inter-element instrumental mass fractionation for Th and U is not simply mass dependant. When the $^{232}Th/^{229}Th$ ratios are normalized for the variable Th/U ratios of the solutions (closed symbols), the data plot along a line with $\beta_{Th} = \beta_U$. It should be noted that the intercept of the $\beta_{Th} = \beta_U$ line is somewhat uncertain because the "true" $^{232}Th/^{229}Th$ ratio is not independently known. (B) A plot of the fractionation-corrected $^{232}Th/^{229}Th$ ratios of the same data as in (A). The fractionation-corrected data (open symbols) display a trend of increasing $^{232}Th/^{229}Th$ ratios with increasing Th/U ratio of the solution. When normalized for this effect, the $^{232}Th/^{229}Th$ ratios agree within analytical uncertainty (closed symbols). (C) A plot of fractionation-corrected $^{232}Th/^{229}Th$ ratios of two aliquots of a Th solution with a constant $^{232}Th/^{229}Th$ ratio of ~ 12. Two portions of this solution were run: one that contained only Th (open symbols) and one that had U from CRM112 added to give a Th/U ratio of ~ 0.8 (closed symbols). The mixed Th–U solution was run in the same fashion as the solution from the first experiment with the final $^{232}Th/^{229}Th$ ratios normalized to Th/U = 0. For the U-free Th solution, the fractionation factor was measured using U from CRM112 before and after each analysis. In this case, the $^{232}Th/^{229}Th$ of the U-free solution was corrected for the effects of instrumental mass fractionation using the average of the two $^{238}U/^{235}U$ ratios (crosses). The average fractionation-corrected $^{232}Th/^{229}Th$ ratios of these two types of measurements are identical within uncertainty (< 0.01% different). The error bars are the average within-run $\pm 2\sigma_m$ uncertainties.

Table 3
Th, U and ^{226}Ra abundances and U-series isotope activity ratios for rock and solution standards by MC-ICP-MS

Standard	#	[Th], μg g^{-1}	[U], μg g^{-1}	Th/U	[^{226}Ra], fg g^{-1}	$\pm 2\sigma_m$ or diff.	%	n=	(^{234}U/^{238}U)	$\pm 2\sigma$	%	n=	(^{230}Th/^{232}Th)	$\pm 2\sigma$ or diff.	%	n=	(^{230}Th/^{238}U)	(^{226}Ra/^{230}Th)
Kil1919	1	1.221	0.4260	2.866					1.0017	0.0023	0.23	4	1.0786	0.0023	0.21	3	1.0186	
	2								1.0013	0.0019	0.18	5	1.0795			1		
	3								1.0010	0.0013	0.13	5	1.0768			1		
	4	1.220	0.4255	2.867	166.8	0.9	0.52	1	1.0015	0.0007	0.07	6	1.0796	0.0037	0.35	7	1.0202	1.1384
	5	1.221	0.4258	2.869	166.7	0.8	0.45	1	1.0018	0.0011	0.11	5						
	6	1.221	0.4264	2.864														
	7	1.228	0.4279	2.870	168.0	1.2	0.71	1	1.0024	0.0017	0.17	3	1.0798	0.0029	0.27	2	1.0214	1.1387
	8								1.0015	0.0018	0.18	3	1.0770	0.0025	0.23	3		
	9	1.223	0.4257	2.872	167.3	0.8	0.49	1	1.0017	0.0023	0.23	2	1.0795	0.0003	0.03	2	1.0219	1.1394
Mean		1.222	0.4262	2.868	167.2				1.0016				1.0787				1.0205	1.1388
$\pm 2\sigma$		0.006	0.0018	0.006	1.2				0.0008				0.0026				0.0029	0.0010
%		0.50	0.42	0.22	0.72				0.08				0.24				0.28	0.09
$\pm 2\sigma_m$		0.002	0.0007	0.003	0.60				0.0003				0.0010				0.0014	0.0006
%		0.20	0.17	0.09	0.42				0.03				0.09				0.14	0.05
n=		6	6	6	4				8				7				4	3
Literature value		1.225	0.4287	2.857	166.9	2.4	1.4	2	1.001				1.083				1.020	1.131
$\pm 2\sigma$ or diff.		0.002	0.001	0.008	2.3				0.002				0.006				0.011	0.016
$\pm 2\sigma_m$		0.001	0.001	0.004									0.004					
n=		5	5	5	2				2				3				1	1
% Diff.		−0.21	−0.58	0.39	0.17				0.06				−0.40				0.05	0.66
TML	1	29.70	10.50	2.827									1.0754	0.0015	0.14	4	1.0019	
(Jar #3)	2	29.74	10.52	2.828	3615	17	0.46	1	1.0002	0.0019	0.19	6	1.0747	0.0007	0.06	3	1.0014	1.0169
	3	29.79	10.54	2.826	3616	30	0.82	1	1.0008	0.0022	0.22	9	1.0733	0.0022	0.22	6	0.9994	1.0168
	4			2.827			0.41	1	1.0000	0.0011	0.11	5	1.0731	0.0034	0.31	5	0.9996	1.0134
	5	29.71	10.51	2.827	3593	20	0.57	1	1.0002	0.0018	0.18	6	1.0721	0.0016	0.15	3	0.9987	1.0143
	6	29.77	10.53	2.826	3612	35	0.97	1	1.0023			1	1.0729	0.0019	0.18	4	0.9992	1.0167
Mean		29.74	10.52	2.827	3609				1.0007				1.0736				1.0001	1.0156
$\pm 2\sigma$		0.08	0.03	0.002	21				0.0019				0.0024				0.0026	0.0032
%		0.26	0.31	0.06	0.59				0.19				0.23				0.26	0.32
$\pm 2\sigma_m$		0.03	0.01	0.001	11				0.0009				0.0011				0.0011	0.0014
%		0.12	0.14	0.02	0.29				0.09				0.10				0.11	0.14
n=		5	5	6	4				5				6				6	5
Nominal value $\pm 2\sigma$									≡ 1.0000 ± 0.0023								≡ 1.0000 ± 0.0048	≡ 1.000 ± 0.015

the precision of Th concentration and $^{232}Th/^{230}Th$ measurements using MC-ICP-MS.

2.10. Summary of our analytical procedures

A typical $^{232}Th/^{230}Th$, $^{226}Ra/^{228}Ra$ or $^{238}U/^{234}U$ analytical session requires measurements of (1) the $^{235}U/^{234}U$ ratio of CRM112, (2) the abundance sensitivity and the shape of the tail (this procedure is only necessary for $^{232}Th/^{230}Th$ ratios), (3) the isobaric interference(s) for the minor isotope(s) and (4) the isotope ratios of the sample. After an analytical session, the final isotope ratio of the sample is (1) corrected for the isobaric interference(s) by subtracting the on-peak baseline(s), (2) normalized to the nominal $^{235}U/^{234}U$ value for CRM112 ($^{232}Th/^{230}Th$ and $^{238}U/^{234}U$ ratios only) and (3) normalized to Th/U = 0 using the relationship in Fig. 6B ($^{232}Th/^{230}Th$ ratios only).

3. Results and discussion

We evaluated the accuracy and precision of our analytical techniques using a range of rock (TML and Kil1919) and solution (UCSC Th "A" and ZSR Th) standards measured over a period of ~ 3 years. Our results are reported in Table 3. In this section, we compare our new MC-ICP-MS data for these standards with literature data collected by mass spectrometry (both MC-ICP-MS and TIMS; Table 4). It should be noted that we switch from atomic to activity ratios for this discussion (the latter are indicated by parentheses and are used to evaluate the presence or absence of radioactive equilibrium between U-series isotopes).

3.1. Accuracy

One test of accuracy is to measure the isotopic composition of Th and/or U solution standards. Our U solution standard, CRM112, cannot be used as a test of accuracy since it was regularly used to correct for variations in the performance of the Daly detector (Fig. 2). Instead, we ran the Th solution standard, UCSC Th "A", which has been analyzed frequently by TIMS. Our average ($^{230}Th/^{232}Th$) ratio for UCSC Th "A" is ~ 0.6% lower than the nominal value for this standard (Table 3) and ~ 0.3–0.6% lower than the range of values previously determined by TIMS (Table 4). Our lower value for UCSC Th "A" lies within the relatively large $\pm 2\sigma$ uncertainties of the TIMS analyses. However, the standard deviation of the mean ($\pm 2\sigma_m$) is probably a better estimate of the analytical uncertainty for a comparison of the average values of a relatively large number of multiple analyses. In this case, our average ($^{230}Th/^{232}Th$) ratio for UCSC Th "A" appears to be distinctly lower than two of the three literature TIMS values listed in Table 3. The origin of this discrepancy is unknown, but it is interesting to note that our value for UCSC Th "A" agrees closely (~ 0.08% different) with the MC-ICP-MS value of Turner et al. (2001).

The analysis of rock standards is another way to explore the accuracy of our analytical techniques. For this purpose, we used a tholeiitic basalt from Kilauea Volcano (Kil1919), which was analyzed previously by

Notes to Table 3:

The accuracy and precision of our Th isotope ratio measurements was evaluated further using the UCSC Th "A" and ZSR Th solution standards. Our average for UCSC Th "A" was ($^{230}Th/^{232}Th$) = 1.0783 ± 0.0023 ($\pm 2\sigma$, $n = 17$), which is 0.62% lower than the nominal value (1.085). Our average for ZSR Th was ($^{230}Th/^{232}Th$) = 0.7991 ± 0.0025 ($\pm 2\sigma$, $n = 24$). The Th, U and ^{226}Ra concentrations are not reported for dissolution #4 of TML-3 because a small amount of sample (~ 1%) was spilled immediately prior to splitting and spiking (this will not affect any of the ratios reported in the table). The other "missing" data are either portions of rock standards that were exhausted during the development of the analytical techniques or rock standards that were analyzed only for Th and U concentrations (Kil1919 #6) or isotope ratios (Kil1919 #2, 3 and 8). The ^{226}Ra concentrations and ($^{226}Ra/^{230}Th$) ratios for Kil11919 are corrected for post-eruptive decay of ^{226}Ra. The age-corrected ^{226}Ra concentration of Kil1919 #5 was calculated from its measured value using the average ($^{230}Th/^{232}Th$) for Kil1919. The literature values and uncertainties for Kil1919 are from Pietruszka et al. (2001). The uncertainties of the single ^{226}Ra concentration measurements are the within-run $\pm 2\sigma_m$ counting statistics. The decay constants used to calculate activity ratios are: $\lambda^{238}U$ (1.551×10^{-10} year^{-1}), $\lambda^{234}U$ (2.826×10^{-6} year^{-1}), $\lambda^{232}Th$ (4.948×10^{-11} year^{-1}), $\lambda^{230}Th$ (9.158×10^{-6} year^{-1}), and $\lambda^{226}Ra$ (4.332×10^{-4} year^{-1}) from Jaffey et al. (1971) for ^{238}U, Cheng et al. (2000) for ^{234}U and ^{230}Th, Le Roux and Glendenin (1963) for ^{232}Th and Tuli (2000) for ^{226}Ra. The $\pm 2\sigma$ errors listed for the nominal (equilibrium) TML values combine the uncertainties of these decay constants with the uncertainties related to the calibration of our ^{233}U, ^{229}Th and ^{228}Ra tracers.

Pietruszka et al. (2001) for Th, U and ^{226}Ra abundances and (^{234}U/^{238}U) and (^{230}Th/^{232}Th) ratios using TIMS. In the following discussion, we directly compare only ratios of the U-series isotopes for Kil1919 because the concentrations may be somewhat variable due to the heterogeneous distribution of Ra-, Th- and U-free olivine in this standard (e.g., Jochum and Hofmann, 1995). Overall, our average (^{234}U/^{238}U), (^{230}Th/^{232}Th), (^{230}Th/^{238}U) and (^{226}Ra/^{230}Th) ratios for Kil1919 agree with the results of Pietruszka et al. (2001) given the relatively large analytical uncertainties of the TIMS data (Table 3). As might be expected

Table 4
Reproducibility of ^{232}Th/^{230}Th, ^{238}U/^{234}U and Th/U ratios and ^{226}Ra concentrations by mass spectrometry

Element(s)	Sample/standard information	Technique	Amount used or sample concentration	Ratio	Reproducibility	n =	Ref.
Th	Solution/rock standards		[Th], ng	^{232}Th/^{230}Th	$\pm 2\sigma$ ($\pm 2\sigma_m$)		
	Th "U"	MC-ICP-MS	100	161,920	1.0% (0.35%)	8	1
	UCSC Th "A"	MC-ICP-MS	75–100	171,660	**0.21% (0.05%)**	17	2
	UCSC Th "A"	MC-ICP-MS	100	171,527	0.57% (0.21%)	7	1
	Kil1919	MC-ICP-MS	75–100	171,600	**0.24% (0.09%)**	19	2
	TML	MC-ICP-MS	600	174,170	0.12% (0.04%)	8	3
	TML	MC-ICP-MS	75–100	172,410	**0.23% (0.09%)**	25	2
	TML	MC-ICP-MS	100	173,010	0.80% (0.30%)	7	1
	L-80-6	MC-ICP-MS	600	175,670	0.10% (0.04%)	8	3
	ATHO	MC-ICP-MS	100	182,150	0.93% (0.38%)	6	1
	Th S1	MC-ICP-MS	5	183,790	1.1% (0.46%)	6	1
	ZSR Th	MC-ICP-MS	75–100	231,640	**0.31% (0.06%)**	24	2
	Cambridge Th "A"	TIMS	400	91,200	0.70% (0.18%)	15	4
	Th "U"	TIMS	≥ 100	163,100	0.69% (0.15%)	22	5
	Th "U"	TIMS	≥ 100	163,500	1.0% (0.24%)	19	6
	UCSC Th "A"	TIMS	50–100	171,100	1.1% (0.18%)	39	7
	UCSC Th "A"	TIMS	?	171,100	1.1% (0.35%)	10	8
	UCSC Th "A"	TIMS	?	170,600	1.5% (0.25%)	35	9
	Th S1	TIMS	100	181,900	1.5% (0.44%)	12	10
Th	Sample replicates		[Th], μg g^{-1}	^{232}Th/^{230}Th	$\pm 2\sigma$ or diff.		
	Kilauea Volcano	TIMS	0.70–1.3	170,100–179,000	0.19–1.4%	6 × 2, 1 × 3	7
	Mid-Atlantic Ridge	TIMS	0.10–0.87	148,600–175,800	0.36–4.6%	7 × 2, 4 × 3	11
	Socorro Island	TIMS	2.3–20	173,400–249,100	0.05–2.8%	11 × 2	9
U	Solution/rock/mineral standards		[U], ng	^{235}U/^{234}U	$\pm 2\sigma$ ($\pm 2\sigma_m$)		
	SRM960 (CRM112-A)	MC-ICP-MS	300–450	137.2	0.13% (0.03%)	19	3
	Kil1919	MC-ICP-MS	20–50	131.9	**0.16% (0.03%)**	33	2
	TML	MC-ICP-MS	20–50	132.1	**0.20% (0.04%)**	27	2
	"Equilib." materials	TIMS	500–3000	132.1	0.08% (0.01%)	36	12
	JR-2	TIMS	100	132.1	0.13% (0.04%)	11	13
	JR-2	TIMS	50	132.2	0.18% (0.05%)	12	13
	SRM960 (CRM112-A)	TIMS	200–600	137.3	0.31% (0.08%)	14	3
	U010	TIMS	50–100	185.5	0.52% (0.16%)	10	7
U	Sample replicates		[U], μg g^{-1}	^{235}U/^{234}U	$\pm 2\sigma$ or diff.		
	Lanzarote Island	TIMS	1.1–1.6	132.3	0.20–0.30%	2 × 2	5
	Kilauea Volcano	TIMS	0.42–0.43	131.1–132.0	0.18–0.83%	2 × 2	7
	Mid-Atlantic Ridge	TIMS	0.036–0.21	130.5–133.0	0.60–3.0%	4 × 2	11

Table 4 (*continued*)

Element(s)	Sample/standard information	Technique	Amount used or sample concentration	Ratio	Reproducibility	$n=$	Ref.
Ra	Rock standard/spl. replicates		[^{226}Ra], fg g^{-1}		$\pm 2\sigma$ or diff.		
	TML	MC-ICP-MS	3600		**0.32%**[a]	1 × 5	2
	Kil1919	MC-ICP-MS	170		**0.09%**[a]	1 × 3	2
	ThITS	TIMS	?		1.3%[a]	1 × 6	16
	Oldoinyo Lengai	TIMS	13,800		1.1%	1 × 3	14
	Mt. Etna	TIMS	1850		0.92%	1 × 2	14
	Mt. Etna	TIMS	1840		1.1%	1 × 6	10
	Mt. Lassen	TIMS	1070		0.47%	1 × 2	15
	Mt. Lassen	TIMS	1070		0.85%	1 × 6	16
	Mt. Lassen	TIMS	1070		1.4%	1 × 2	5
	Karthala Volcano	TIMS	820		0.61%	1 × 2	14
	Iceland	TIMS	450		0.08%	1 × 4	17
	Tonga–Kermadec Arc	TIMS	50–230		0.13–3.6%	4 × 2	16
	Kilauea Volcano	TIMS	90–170		0.65–1.5%	4 × 2	7
	Iceland	TIMS	70–90		1.7–2.2%	2 × 2	17
	Mid-Atlantic Ridge	TIMS	20–90		1.1–8.2%	7 × 2	11
	"Mid-ocean"	TIMS	10–70		1.9–3.6%	2 × 2	15
Th, U	Rock standard/spl. replicates		[Th], μg g^{-1}	Th/U	$\pm 2\sigma$ or diff.		
	TML-3	MC-ICP-MS	30	2.8	**0.06%**	1 × 6	2
	Kil1919	MC-ICP-MS	1.2	2.9	**0.22%**	1 × 6	2
	Gaussberg Volcano	TIMS	25–30	7.2–7.7	0.03–0.43%	3 × 2	18
	ATHO	TIMS	7.4	3.3	0.43%	1 × 4	19
	Kil1919	TIMS	1.2	2.9	0.28%	1 × 5	7
	Ardoukoba Volcano	TIMS	0.39–0.91	3.7	0.32–1.7%	4 × 2	20
	Mid-Atlantic Ridge	TIMS	0.10–0.76	2.8–3.3	0.84–4.9%	7 × 2, 1 × 3	11
	Mid-Atlantic Ridge	TIMS	0.08–0.15	2.7–3.1	0.11–3.3%	4 × 2	19

Th and U isotope ratio data collected by TIMS from solution and rock standards are summarized only for $n \geq 10$. Under the column "$n=$", a single number indicates the number of replicate analyses of a given standard, whereas the format A × B indicates the number of different standards or samples (A) that were analyzed a given number of times (B). The reproducibility is calculated either as the % difference ($n=2$) or $\pm 2\sigma$ ($\pm 2\ \sigma_m$) variation of the data in % ($n>2$). References: (1) Turner et al. (2001), (2) this study (**bold**), (3) Luo et al. (1997), (4) Cohen and O'Nions (1993), (5) Thomas et al. (1999), (6) Turner et al. (1997), (7) Pietruszka et al. (2001 and related unpubl. metadata), (8) Reid and Ramos (1996), (9) Bohrson and Reid (1998), (10) Claude-Ivanaj et al. (1998), (11) Lundstrom et al. (1998), (12) Cheng et al. (2000), (13) Yokoyama et al. (2001), (14) Chabaux et al. (1994), (15) Volpe et al. (1991), (16) Turner et al. (2000), (17) Cohen and O'Nions (1991), (18) Williams et al. (1992), (19) Peate et al. (2001) and (20) Vigier et al. (1999).

[a] Reproducibility based on (^{226}Ra/^{230}Th) ratios rather than ^{226}Ra concentrations.

from the ~ 0.3% difference in the (^{230}Th/^{232}Th) ratio of the UCSC Th "A" standard between the two laboratories (Table 4), our average (^{230}Th/^{232}Th) ratio for Kil1919 is slightly (~ 0.4%) lower than the value of Pietruszka et al. (2001). However, only the Th/U ratios are significantly different between the two laboratories outside of the $\pm 2\sigma_m$ uncertainties, which may reflect small errors (adding up to ~ 0.4% difference) in the concentrations of the Th and U standards used to calibrate the ^{229}Th and ^{233}U tracers.

The strongest test of accuracy for the measurement of U-series isotopes is the analysis of a material that is thought to be in radioactive equilibrium. For this purpose, we used the Pliocene rock standard TML (Jar #3). Given the old age of TML compared to the half-lives of ^{226}Ra (1600 years), ^{230}Th (~ 75 ka) and ^{234}U (~ 245 ka), this standard is thought to be in ^{226}Ra–^{230}Th–^{234}U–^{238}U radioactive equilibrium (Williams et al., 1992). Thus, the (^{234}U/^{238}U), (^{230}Th/^{238}U) and (^{226}Ra/^{230}Th) ratios of this standard

should equal unity within the uncertainty of the calibration of our ^{228}Ra, ^{229}Th and ^{233}U tracers (for ^{230}Th–^{238}U and ^{226}Ra–^{230}Th) and/or the decay constants (for all three isotope pairs). However, it is important to note that TML is thought to be heterogeneous with respect to its (^{230}Th/^{232}Th) and Th/U ratios (Williams et al., 1992). Thus, a comparison of our results for these ratios with other laboratories is not particularly meaningful. Overall, our average $\pm 2\sigma$ results for (^{234}U/^{238}U), (^{230}Th/^{238}U) and (^{226}Ra/^{230}Th) for TML are identical to equilibrium within the uncertainties of the decay constants and the errors associated with the calibration of our ^{229}Th, ^{233}U and ^{228}Ra tracers (Table 3). Furthermore, our average (^{234}U/^{238}U) and (^{230}Th/^{238}U) ratios for TML equal unity within the smaller $\pm 2\sigma_m$ errors of the replicate analyses ($\sim 0.1\%$ each), which attests to the accuracy of the new decay constants proposed for ^{230}Th and ^{234}U (Cheng et al., 2000). In contrast, our average (^{226}Ra/^{230}Th) for TML is measurably different from unity at the $\pm 2\sigma$ and $\pm 2\sigma_m$ levels of the replicate analyses (although still within the $\pm 2\sigma$ uncertainty of the equilibrium value). This is somewhat unsatisfying, but we do not regard the elevated ^{226}Ra content of TML to be significant due to the relatively large overall uncertainty in the concentration of our ^{226}Ra standard (1.2%).

3.2. Precision

Overall, the $\pm 2\sigma$ reproducibilities of our (^{234}U/^{238}U) and (^{230}Th/^{232}Th) measurements by MC-ICP-MS are $\sim 0.2\%$ ($n=60$) and $\sim 0.3\%$ ($n=85$), respectively (Fig. 7). This is $\sim 2-3\times$ less precise than the data reported by Luo et al. (1997) using similar MC-ICP-MS techniques (Table 4). The origin of this difference is unknown, but may partly reflect the larger number of standards analyzed in our study. For example, the $\pm 2\sigma_m$ uncertainties of the two studies are more similar (less than a factor of ~ 2 different; Table 4). Using sample sizes that are similar to the requirements of state-of-the-art TIMS, we are able to measure (^{230}Th/^{232}Th) ratios with a precision that is at least $\sim 2-3\times$ better than TIMS (Table 4) and (^{234}U/^{238}U) ratios with a precision that is comparable to TIMS (the latter is based on a comparison with TIMS data collected using similar amounts of U; Table 4). Furthermore, it is important to note that the

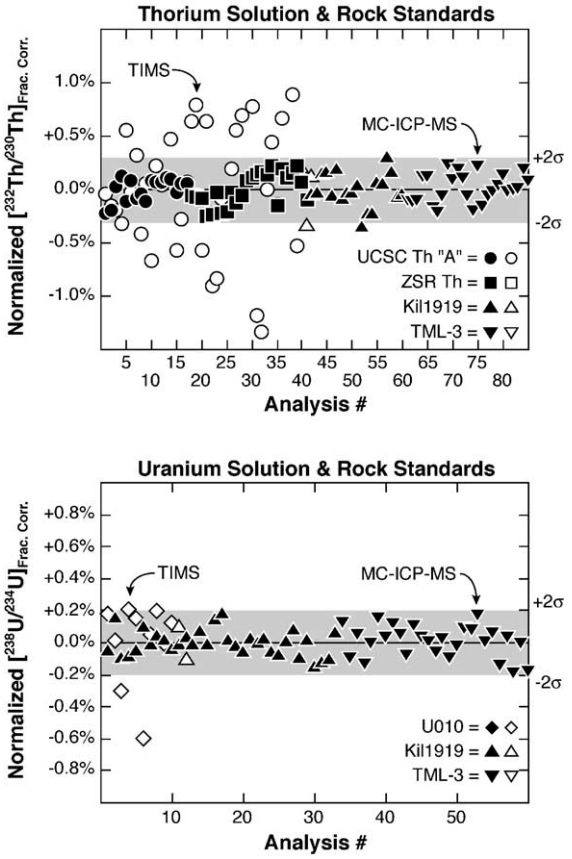

Fig. 7. Precision of our ^{232}Th/^{230}Th and ^{238}U/^{234}U measurements by MC-ICP-MS (closed symbols) compared to TIMS (open symbols) using several different rock and solution standards. For comparison, the results for each standard are normalized to its average value and plotted as the % deviation from this average. The $\pm 2\sigma$ within-run errors for the MC-ICP-MS data are similar to or less than the long-term external reproducibility of the ^{232}Th/^{230}Th and ^{238}U/^{234}U ratios ($\sim 0.3\%$ and 0.2%, respectively). The TIMS data are from Pietruszka et al. (2001 and related unpubl. metadata).

reproducibility of our (^{230}Th/^{232}Th) and (^{234}U/^{238}U) measurements using MC-ICP-MS is identical for both matrix-free solution standards and multiple preparations of both high- and low-concentration rock standards (Fig. 7). In contrast, replicate Th and U isotope ratio measurements of volcanic rocks by TIMS may have a reproducibility that is up to $\sim 2-5\times$ worse than would be expected from multiple analyses of solution standards (Table 4).

Although it is important to obtain high-quality measurements of (^{230}Th/^{232}Th) ratios for U-series

isotope studies of active volcanoes, precise measurements of $^{230}Th-^{238}U$ disequilibria in volcanic rocks require a similar reproducibility for Th/U ratios. The precision of our Th/U measurements by MC-ICP-MS was evaluated using multiple preparations of the rock standards Kil1919 ($n=6$) and TML ($n=6$). These results show a reproducibility of $\sim 0.2\%$ ($\pm 2\sigma$), which is similar to or slightly better than the precision of the highest quality TIMS data (Table 4). It is important to note that this high precision was attained without the use of $HClO_4$ or boric acid, which are frequently used by other laboratories during sample dissolution to ensure complete equilibration between the sample and spike. We estimate the $\pm 2\sigma$ precision of our MC-ICP-MS techniques for the measurement of $^{230}Th-^{238}U$ disequilibria at $\sim 0.3\%$ based on multiple analyses of Kil1919 and TML (Table 3). This reproducibility is consistent with the overall precision of our Th/U and ($^{230}Th/^{232}Th$) measurements ($\sim 0.2\%$ and 0.3%, respectively) and translates directly to a precision for $^{230}Th-^{238}U$ disequilibria that is at least $\sim 2-3\times$ better than TIMS.

The precision of our $^{226}Ra-^{230}Th$ disequilibria measurements by MC-ICP-MS was evaluated using multiple preparations of the rock standards Kil1919 ($n=3$) and TML ($n=5$). Our results indicate a $\pm 2\sigma$ re-producibility for $^{226}Ra-^{230}Th$ disequilibria of $\sim 0.3\%$ (Table 3). Although few TIMS laboratories have directly evaluated the precision of their measurements of $^{226}Ra-^{230}Th$ disequilibria, this is at least $\sim 2-3\times$ better than the reproducibility of most replicate analyses of ^{226}Ra abundances in volcanic rocks by TIMS (Table 4). However, it is important to note that the true precision of $^{226}Ra-^{230}Th$ disequilibria measurements should also include the reproducibility of the ($^{230}Th/^{232}Th$) ratios and Th concentrations (which is rarely evaluated). If these were included, the overall precision of our measurements of $^{226}Ra-^{230}Th$ disequilibria by MC-ICP-MS would be expected to be even better than TIMS (given the higher precision of Th isotope ratio measurements by MC-ICP-MS).

4. Conclusions

In this paper, we have described new analytical techniques for the precise and accurate measurement of $^{226}Ra-^{230}Th-^{238}U$ disequilibria in volcanic rocks using MC-ICP-MS. The greatest strength of our MC-ICP-MS methods is the higher precision compared to TIMS (at least $\sim 2-3\times$ better using sample sizes that are similar to the requirements of state-of-the-art TIMS). However, there are several weaknesses to our analytical techniques for ^{230}Th and ^{226}Ra that could be improved substantially by future studies, such as (1) the magnitude of the correction for the tail of ^{232}Th beneath ^{230}Th, (2) the lower sensitivity for Ra by MC-ICP-MS ($\sim 0.5\pm 0.1\%$ in this study) compared to TIMS ($\sim 10-15\%$ for pure standards, but $\sim 2\times$ lower for samples; Cohen and O'Nions, 1991), (3) the software limitation that requires the use of ^{235}U (rather than ^{238}U) to correct the $^{226}Ra/^{228}Ra$ ratio for fluctuations in the signal intensity and (4) the requirement of a third measurement sequence for $^{226}Ra/^{228}Ra$ measurement due to problems setting the Faraday collectors at 1 amu spacing (Fig. 1). However, it is important to note that these "problems" for MC-ICP-MS are more than offset by the much higher sensitivity for Th compared to TIMS and the ability to correct the measured $^{232}Th/^{230}Th$ and $^{226}Ra/^{228}Ra$ ratios for the effects of instrumental mass fractionation and/or variations in the Daly–Faraday gain using the $^{238}U/^{235}U$ ratio of a natural U standard added to the sample (impossible by TIMS). These analytical improvements will increase the usefulness of U-series isotopes as high-resolution tracers of the nature and timing of magmatic processes at active volcanoes.

Acknowledgements

This development work was conducted while the first author was a Carnegie Postdoctoral Research Fellow at DTM. The creative advice of M. Horan and T. Mock helped us to surmount a number of vexing analytical challenges related to the chemistry and mass spectrometry. We are very grateful to both of them. D. Snyder conducted analysis #6 of the TML rock standard as part of his dissertation research project at DTM. We also thank M. Garcia, J. Gill, S. Hart, P. Holden, K. Rubin and K. Sims for providing some of the isotopic spikes and/or rock and solution standards used in this project. The critical comments of S. Turner and an anonymous

reviewer helped us to focus the presentation of our results. **[RR]**

References

Bohrson, W.A., Reid, M.R., 1998. Genesis of evolved ocean island magmas by deep- and shallow-level basement recycling, Socorro Island, Mexico: constraints from Th and other isotope signatures. J. Petrol. 39, 995–1008.

Carlson, R.W., Hauri, E.H., Alexander, C.M.O.D., 2001. Matrix induced isotopic mass fractionation in the ICP-MS. In: Holland, G.P., Tanner, S.D. (Eds.), Plasma Source Mass Spectrometry: The New Millennium. The Royal Society of Chemistry, Cambridge, pp. 288–297.

Chabaux, F., Ben Othman, D., Birck, J.L., 1994. A new Ra–Ba chromatographic separation and its application to Ra mass-spectrometric measurement in volcanic rocks. Chem. Geol. 114, 191–197.

Cheng, H., Edwards, R.L., Hoff, J., Gallup, C.D., Richards, D.A., Asmerom, Y., 2000. The half-lives of uranium-234 and thorium-230. Chem. Geol. 169, 17–33.

Claude-Ivanaj, C., Bourdon, B., Allègre, C.J., 1998. Ra–Th–Sr isotope systematics in Grande Comore Island: a case of plume–lithosphere interaction. Earth Planet. Sci. Lett. 164, 99–117.

Cohen, A.S., O'Nions, R.K., 1991. Precise determination of femtogram quantities of radium by thermal ionization mass spectrometry. Anal. Chem. 63, 2705–2708.

Cohen, A.S., O'Nions, R.K., 1993. Melting rates beneath Hawaii: evidence from uranium series isotopes in recent lavas. Earth Planet. Sci. Lett. 120, 169–175.

Edwards, R.L., Chen, J.H., Wasserburg, G.J., 1987. ^{238}U–^{234}U–^{230}Th–^{232}Th systematics and the precise measurement of time over the past 500,000 years. Earth Planet. Sci. Lett. 81, 175–192.

Goldstein, S.J., Murrell, M.T., Janecky, D.R., 1989. Th and U isotopic systematics of basalts from the Juan de Fuca and Gorda Ridges by mass spectrometry. Earth Planet. Sci. Lett. 96, 134–146.

Halliday, A.N., Lee, D.-C., Christensen, J.N., Rehkämper, M., Yi, W., Luo, X., Hall, C.M., Ballentine, C.J., Pettke, T., Stirling, C., 1998. Applications of multiple collector-ICPMS to cosmochemistry, geochemistry, and paleoceanography. Geochim. Cosmochim. Acta 62, 919–940.

Horwitz, E.P., Chiarizia, R., Dietz, M.L., 1992. A novel strontium-selective extraction chromatographic resin. Solvent Extr. Ion Exch. 10, 313–336.

Horwitz, E.P., Chiarizia, R., Dietz, M.L., Diamond, H., Nelson, D.M., 1993. Separation and preconcentration of actinides from acidic media by extraction chromatography. Anal. Chim. Acta 281, 361–372.

Jaffey, A.H., Flynn, K.F., Glendenin, L.E., Bentley, W.C., Essling, A.M., 1971. Precison measurement of half-lives and specific activities of ^{235}U and ^{238}U. Phys. Rev. 4, 1889–1906.

Jochum, K.P., Hofmann, A.W., 1995. Contrasting Th/U in historical Mauna Loa and Kilauea lavas. In: Rhodes, J.M., Lockwood, J.P. (Eds.), Mauna Loa Revealed: Structure, Composition, History, and Hazards. AGU Geophys. Monogr., vol. 92, pp. 307–314.

Le Roux, L.J., Glendenin, L.E., 1963. Half-live of thorium-232. Proc. of the National Conference on Nuclear Energy, Pretoria, South Africa, 83–94.

Lundstrom, C.C., Gill, J., Williams, Q., Hanan, B.B., 1998. Investigating solid mantle upwelling beneath mid-ocean ridges using U-series disequilibria: II. A local study at 33°S Mid-Atlantic Ridge. Earth Planet. Sci. Lett. 157, 167–181.

Luo, X., Rehkämper, M., Lee, D.-C., Halliday, A.N., 1997. High precision $^{230}Th/^{232}Th$ and $^{234}U/^{238}U$ measurements using energy-filtered magnetic sector multiple collector mass spectrometry. Int. J. Mass Spectrom. Ion Processes 171, 105–117.

Maréchal, C.N., Télouk, P., Albarède, F., 1999. Precise analysis of copper and zinc isotopic compositions by plasma-source mass spectrometry. Chem. Geol. 156, 251–273.

McDermott, F., Elliott, T.R., van Calsteren, P., Hawkesworth, C.J., 1993. Measurement of $^{230}Th/^{232}Th$ ratios in young volcanic rocks by single-sector thermal ionization mass spectrometry. Chem. Geol. 103, 283–292.

Oversby, V.M., Gast, P.W., 1968. Lead isotope compositions and uranium decay series disequilibrium in recent volcanic rocks. Earth Planet. Sci. Lett. 5, 199–206.

Peate, D.W., Hawkesworth, C.J., van Calsteren, P.W., Taylor, R.N., Murton, B.J., 2001. ^{238}U–^{230}Th constraints on mantle upwelling and plume–ridge interaction along the Reykjanes Ridge. Earth Planet. Sci. Lett. 187, 259–272.

Pietruszka, A.J., Rubin, K.H., Garcia, M.O., 2001. ^{226}Ra–^{230}Th–^{238}U disequilibria of historical Kilauea lavas (1790–1982) and the dynamics of mantle melting within the Hawaiian plume. Earth Planet. Sci. Lett. 186, 15–31.

Reid, M.R., Ramos, F.C., 1996. Chemical dynamics of enriched mantle in the southwestern United States: thorium isotope evidence. Earth Planet. Sci. Lett. 138, 67–81.

Russell, W.A., Papanastassiou, D.A., Tombrello, T.A., 1978. Ca isotope fractionation on the Earth and other solar system materials. Geochim. Cosmochim. Acta 42, 1075–1090.

Somayajulu, B.L.K., Tatsumoto, M., Rosholt, J.N., Knight, R.J., 1966. Disequilibrium of the ^{238}U series in basalt. Earth Planet. Sci. Lett. 1, 387–391.

Thomas, L.E., Hawkesworth, C.J., van Calsteren, P., Turner, S.P., Rogers, N.W., 1999. Melt generation beneath ocean islands: a U–Th–Ra isotope study from Lanzarote in the Canary Islands. Geochim. Cosmochim. Acta 63, 4081–4099.

Tuli, J.K., 2000. Nuclear Wallet Cards. Brookhaven National Laboratory, New York, 114 pp.

Turner, S., Hawkesworth, C., Rogers, N., King, P., 1997. U–Th isotope disequilibria and ocean island basalt generation in the Azores. Chem. Geol. 139, 145–164.

Turner, S., Bourdon, B., Hawkesworth, C., Evans, P., 2000. ^{226}Ra–^{230}Th evidence for multiple dehydration events, rapid melt ascent and the time scales of differentiation beneath the Tonga–Kermadec island arc. Earth Planet. Sci. Lett. 179, 581–593.

Turner, S., van Calsteren, P., Vigier, N., Thomas, L., 2001. Determination of thorium and uranium isotope ratios in low-concen-

tration geological materials using a fixed multi-collector-ICP-MS. J. Anal. At. Spectrom. 16, 612–615.

Vigier, N., Bourdon, B., Joron, J.L., Allègre, C.J., 1999. U-decay series and trace element systematics in the 1978 eruption of Ardoukoba, Asal rift: timescale of magma crystallization. Earth Planet. Sci. Lett. 174, 81–97.

Volpe, A.M., Olivares, J.A., Murrell, M.T., 1991. Determination of radium isotope ratios and abundances in geologic samples by thermal ionization mass spectrometry. Anal. Chem. 63, 913–916.

Walder, A.J., Platzner, I., Freedman, P.A., 1993. Isotope ratio measurement of lead, neodymium, and neodymium–samarium mixtures, hafnium and hafnium–lutetium mixtures with a double focusing multiple collector inductively coupled plasma mass spectrometer. J. Anal. At. Spectrom. 8, 19–23.

White, W.M., Albarède, F., Télouk, P., 2000. High-precision analysis of Pb isotope ratios by multi-collector ICP-MS. Chem. Geol. 167, 257–270.

Williams, R.W., Collerson, K.D., Gill, J.B., Deniel, C., 1992. High Th/U ratios in subcontinental lithospheric mantle: mass spectrometric measurement of Th isotopes in Gaussberg lamproites. Earth Planet. Sci. Lett. 111, 257–268.

Yokoyama, T., Makishima, A., Nakamura, E., 2001. Precise analysis of $^{234}U/^{238}U$ ratio using UO_2^+ ion with thermal ionization mass spectrometry for natural samples. Chem. Geol. 181, 1–12.